Theory Biosci. (2010) 129:25–38
DOI 10.1007/s12064-010-0080-1

ORIGINAL PAPER

Jensen's inequality as a tool for explaining the effect of oscillations on the average cytosolic calcium concentration

Beate Knoke · Christian Bodenstein · Marko Marhl · Matjaž Perc · Stefan Schuster

Received: 18 December 2009 / Accepted: 21 January 2010 / Published online: 16 February 2010

Abstract It has often been asked which physiological advantages calcium (Ca^{2+}) oscillations in non-excitable cells may have as compared to an adjustable stationary Ca^{2+} signal. One of the proposed answers is that an oscillatory regime allows a lowering of the average Ca^{2+} concentration, which is likely to be advantageous because Ca^{2+} is harmful to the cell in high concentrations. To check this hypothesis, we apply Jensen's inequality to study the relation between the average Ca^{2+} concentration during oscillations and the Ca^{2+} concentration at the (unstable) steady state. Jensen's inequality states that for a (strictly) convex function, the function value of the average of a set of argument values is lower than the average of the function values of the arguments from that set. We show that the kinetics of the Ca^{2+} efflux out of the cell is crucial in this context. By analytical calculations we derive that, if the Ca^{2+} efflux is a convex function of the cytosolic Ca^{2+} concentration, then oscillations lower the average Ca^{2+} concentration in comparison to the unstable steady state. If it is a concave function, the average Ca^{2+} concentration is increased, while it remains the same if that function is linear. We also analyse the case where the efflux obeys a Hill kinetics, which involves both a convex and a concave part. The results are illustrated by numerical simulations and simple example models. The theoretical predictions are tested with three experimental data sets from the literature. In two of them, the average appears to be higher than the steady-state value, while the third points to approximate equality. Thus oscillations may be used in real cells to tune the average Ca^{2+} concentration in both directions.

Keywords Calcium oscillations · Jensen's inequality · Average calcium concentration · Convex function · Concave function · Hill kinetics · Advantage of oscillations

B. Knoke · C. Bodenstein · S. Schuster (✉)
Department of Bioinformatics, Friedrich Schiller University Jena, Ernst-Abbe-Platz 2, 07743 Jena, Germany
e-mail: stefan.schu@uni-jena.de

B. Knoke
e-mail: bknoke@gmx.org

C. Bodenstein
e-mail: christian.bodenstein@uni-jena.de

M. Marhl · M. Perc
Department of Physics, Faculty of Natural Sciences and Mathematics, University of Maribor, Koroška cesta 160, 2000 Maribor, Slovenia
e-mail: marko.marhl@uni-mb.si

M. Perc
e-mail: matjaz.perc@uni-mb.si

Present Address:
B. Knoke
Institute of Biochemical Engineering, University of Stuttgart, Allmandring 31, 70569 Stuttgart, Germany

List of symbols

K	Dissociation constant of CICR
k_2	Rate constant of pumping Ca^{2+} from the cytosol into the intracellular stores
k_3	Rate constant of CICR
k_f	Rate constant of the leak efflux
K_S	Half-saturation constant
n	Hill coefficient
t	Time
$f(Z)$	Vout efflux function out of the cell
V_{in}	Influx function into the cell
V_{pump}	ATPase pumping Ca^{2+} from the cytosol into the intracellular stores
V_{CICR}	Ca^{2+} release out of the ER following the CICR
V_{leak}	Leak flux out of the intracellular stores

Y	Overall concentration of Ca^{2+} in the intracellular stores
Y_i	Concentration of Ca^{2+} in one of the intracellular stores
Z	Concentration of Ca^{2+} in the cytosol
Z_{ss}	Steady-state concentration of Ca^{2+} in the cytosol
$\langle Z \rangle$	Average concentration of Ca^{2+} in the cytosol

Abbreviations

CaM	Calmodulin
CICR	Ca^{2+}-induced Ca^{2+} release mechanism
ER	Endoplasmic reticulum
IP_3	Inositol-1,4,5-trisphosphate
PMCA	Plasma membrane Ca^{2+} ATPase
SOCs	Store-operated Ca^{2+} channels

Subscripts

m	Mitochondria
ER	Endoplasmic reticulum

Introduction

Oscillations in the concentration of cytosolic calcium ions are of importance in intracellular signal transduction. For more than two decades, Ca^{2+} oscillations in non-excitable cells such as oocytes, hepatocytes and astrocytes have been the subject of extensive experimental (e.g. Woods et al. 1986; Dupont et al. 2000; Bruce et al. 2003; Berridge et al. 2003; Thul et al. 2008) and theoretical work (cf. Goldbeter 1996; Schuster et al. 2002; Falcke 2004; Dupont et al. 2007). Depending on experimental conditions, Ca^{2+} oscillations show different time courses. While they are sometimes sinusoidal (Szekely et al. 2009), usually spike-like oscillations are observed (for experimental traces, see Rooney et al. 1989; Somogyi and Stucki 1991; Li et al. 1994).

It has often been asked which physiological advantages Ca^{2+} oscillations have in comparison to adjustable stationary concentrations (Jacob 1990; Heinrich and Schuster 1996; Dupont and Goldbeter 1998; Putney 1998; Gall et al. 2000; Schuster et al. 2002; Knoke et al. 2008). It was suggested that lowering the cytosolic Ca^{2+} concentration could be an advantage of oscillations (Berridge 1989; Gall et al. 2000; Schuster et al. 2002), since high sustained concentrations are harmful for the cell due to precipitation of Ca^{2+} salts or initiation of apoptosis by Ca^{2+} overloaded mitochondria (Berridge 1997; Berridge et al. 1998). This calls for a strictly controlled Ca^{2+} homeostasis with very low (≈ 0.1 μM) basal cytosolic Ca^{2+} concentrations (Berridge et al. 2003), as was also discussed for reactive oxygen species (Hauser et al. 2001; Olsen et al. 2003). This (hitherto unproven) hypothesis is the motivation for us to study the relation between the average Ca^{2+} concentration during oscillations and the Ca^{2+} concentration at the (unstable) steady state. We have shown earlier that many models of Ca^{2+} oscillations have the property that the average concentration equals the concentration at the (unstable) steady state rather than to be lower (Knoke et al. 2008). This equality property holds if the following three conditions are fulfilled:

(a) There is an exchange of Ca^{2+} across the cell membrane.
(b) The net Ca^{2+} flow across the cell membrane contains a positive constant influx and an efflux proportional to the cytosolic Ca^{2+} concentration. (If the influx is reversible, we can formally include the backward flow into the efflux.)
(c) The fluxes mentioned in condition (b) do not depend on any other concentration variables in the model (for example, Ca^{2+} in the intracellular stores and of Ca^{2+} bound to proteins).

An interpretation of these conditions, (analytical and numerical) calculations for several models that fulfil these conditions, and a generalisation to other biological oscillators were given earlier (Knoke et al. 2008). In view of a later modification with a non-linear dependence of the net flow on cytosolic Ca^{2+}, condition (b) can be decomposed into two conditions:

(b1) The forward flow of the Ca^{2+} influx is independent of the cytosolic Ca^{2+} concentration.
(b2) The Ca^{2+} efflux (possibly including the backward flow of a reversible influx) is proportional to the cytosolic Ca^{2+} concentration.

Due to conditions (b1) and (c), the unidirectional Ca^{2+} influx must be independent of any model variable, while it can depend on parameters such as hormone concentrations and the external Ca^{2+} concentration, which is usually regarded as a constant due to the larger volume of the extracellular space.

Since rate laws relevant in cell biology are usually non-linear, it is questionable whether condition (b2) is fulfilled in real systems. In fact, it was experimentally observed that the Ca^{2+} efflux in many cell types obeys Hill kinetics, for example, in human embryonic kidney (HEK) cells (Albrecht et al. 2002). This has been used in a corresponding model (Szekely et al. 2009). Also in pancreatic acinar cells (Camello et al. 1996) and erythrocytes (in which, however, no sustained Ca^{2+} oscillations occur) (Carafoli 1991b; Valant et al. 1992) the Ca^{2+} efflux is best described by a sigmoidal Hill function. For hepatocytes, several studies are indicative of Michaelis–Menten kinetics (Lin 1985; Birch-Machin and Dawson 1988; Evers et al. 1988; Kessler et al. 1990). The question arises how the average

Ca^{2+} concentration is affected by oscillations in such cases. This is interesting in view of elucidating the potential physiological advantages of oscillatory behaviour of Ca^{2+} and, thus, tackling the question why such oscillations have emerged during evolution. We address this question in the present paper by dropping condition (b2).

It should be noted that also other potential advantages of oscillations have been discussed (cf. Schuster et al. 2002), such as higher robustness against perturbations (Rapp et al. 1981; Gall et al. 2000) and prevention of receptor desensitisation (Jacob 1990). In the present paper, however, we focus on the effect of oscillations on the average Ca^{2+} concentration. It turns out that Jensen's inequality (Jensen 1906; cf. Krantz 1999) provides a well-suited mathematical background.

Methods

Mathematical background

As a start, we briefly recapitulate Jensen's inequality property for convex and concave functions (Jensen 1906) before going into the analytical calculations for the Ca^{2+} models. That inequality (published in French) is named after Danish mathematician Johan Jensen. It says that a convex function has the property that the function value of the average (of two or more) argument values Z_1, Z_2, … forming a set $\mathbf{Z}$ is not greater than the average of the function values $f(\mathbf{Z})$ (see Fig. 1 and cf. Hardy et al. 1988; Krantz 1999). Already in the original paper by Jensen (1906), the inequality was also formulated for the measure-theoretic case where $\mathbf{Z}$ is a continuous interval. For the analysis of Ca^{2+} oscillations, this case is relevant. The variable Z is then the cytosolic Ca^{2+} concentration, which is a periodic function of time. For obvious reasons, we consider the average over one (or several) periods of the oscillation, which can be expressed as an integral over time divided by the oscillation period T:

$$f\left(\frac{\int_T Z(t)\mathrm{d}t}{T}\right) \leq \frac{\int_T f(Z(t))\mathrm{d}t}{T}, \tag{1}$$

with f being convex over an interval $\mathbf{Z}$ between minimum and maximum values (amplitudes) of the oscillation. Using the short notation for the average $\langle\rangle$ this can be written as:

$$f(\langle Z\rangle) \leq \langle f(Z)\rangle. \tag{2}$$

For strictly convex functions the inequality in relation 1 is strict. For concave functions, the opposite holds:

$$f(\langle Z\rangle) \geq \langle f(Z)\rangle. \tag{3}$$

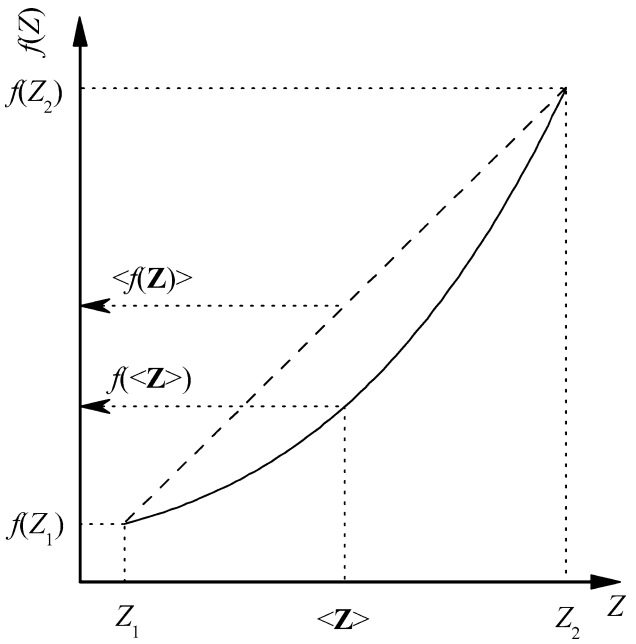

Fig. 1 Illustration of Jensen's inequality by using a set $\mathbf{Z}$ of just two values, Z_1 and Z_2. $\langle f(\mathbf{Z})\rangle$ is the average of the function values, while $f(\langle\mathbf{Z}\rangle)$ is the function value of the averaged argument. The *thick solid curve* is the convex function $f(Z)$. The *dashed line* connects the function values of Z_1 and Z_2 to visualise the average of these function values

with an analogous constraint for strictly concave functions.

The prerequisite of convexity for Jensen's inequality to be true is that the second derivative of $f(Z)$ is non-negative, $f''(Z) \geq 0$, for all Z in an interval comprising $\mathbf{Z}$.

Model describing the generation of Ca^{2+} oscillations

Now we describe a general oscillation model complying with the conditions (a), (b1) and (c) given in the "Introduction" section. As mentioned in the "Introduction" section, we drop condition (b2) and allow the efflux to be a non-linear function of cytosolic Ca^{2+}. This model will be used in the present article for demonstrating the usefulness of Jensen's inequality in the analysis of Ca^{2+} oscillations. Special cases of that model are, for example, the models proposed by Li et al. (1994) and Sneyd et al. (2004). Höfer (1999) used a similar model for analysing the coupling between cells. When the exchange across gap junctions is neglected, the Höfer model simplifies to one in which conditions (a), (b1) and (c) are fulfilled and the efflux follows a Hill kinetics with a Hill coefficient of 2. Moreover, the models of Somogyi and Stucki (1991), Goldbeter et al. (1990), Dupont and Goldbeter (1993), which fulfil conditions (a)–(c), could be modified by taking a non-linear rate for the efflux.

Let $Z(t)$ and $Y(t)$ denote the concentrations of Ca^{2+} in the cytosol and intracellular stores at time t, respectively. Then, the system equations can be written as

$$\frac{dZ}{dt} = V_{in} - V_{pump} + V_{CICR} + V_{leak} - f(Z) \quad (4)$$

$$\frac{dY}{dt} = V_{pump} - V_{CICR} - V_{leak} \quad (5)$$

with a constant influx into the cell, $V_{in} = \text{const.}$, and $f(Z)$ denoting the efflux out of the cell. V_{pump}, V_{CICR} and V_{leak} denote the rates of the ATPase pumping Ca^{2+} from the cytosol into the intracellular stores, the Ca^{2+} release out of the stores through specific channels following the Ca^{2+}-induced Ca^{2+} release (CICR) mechanism (cf. Goldbeter 1996) and the leak flux out of the stores, respectively (Fig. 2).

Knowledge of the kinetics of these exchange fluxes between the cytosol and stores is not necessary for the analytical derivation in the "General derivation" section, since Eqs. 4 and 5 sum up to the general equation:

$$\frac{d(Y+Z)}{dt} = V_{in} - f(Z). \quad (6)$$

In contrast, for the numerical simulations in the "Numerical simulations by way of examples" section, we will specify the kinetics of the exchange fluxes. The differential equation system 4 and 5 may include more than two variables, as long as they do not influence any influx or efflux term of Ca^{2+} across the cell membrane (see condition c). The additional substances are then not relevant for analysing the average of cytosolic Ca^{2+}. Such a substance could be, for example, inositol trisphosphate (IP_3), which was considered in a three-variable model proposed by Borghans et al. (1997) and analysed further by Houart et al. (1999). That model does fulfil the three conditions (a)–(c). A further generalisation of Eqs. 4 and 5 is that several various intracellular stores exist, so that several variables Y_i should be considered (Fig. 2). For example in the first two models considered in Grubelnik et al. (2001), mitochondrial Ca^{2+} uptake and release was included. An equation analogous to Eq. 6 can then be derived easily.

The numerical solutions of differential equations are here obtained by using the software MADONNA (University of Berkeley, CA) with the Rosenbrock (stiff) integration method.

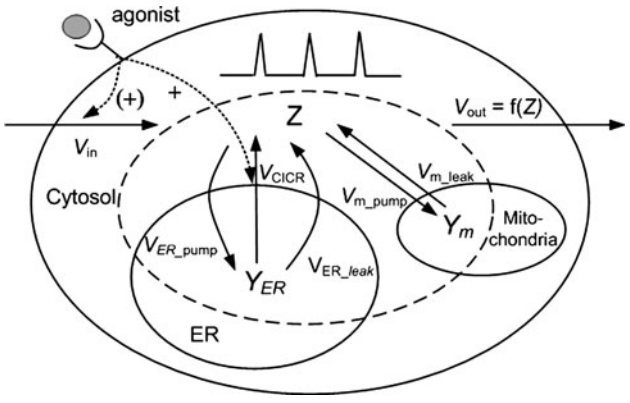

Fig. 2 Scheme of the Ca^{2+} oscillation model used in this study. *Ellipses* indicate membranes. For symbols, see list of abbreviations

Results

General derivation

We now compare, in a general way, the average concentration of cytosolic Ca^{2+} to that at the (unstable) steady state for models satisfying conditions (a), (b1) and (c) given in the "Introduction" section. Equation 6 implies that Ca^{2+} in the cytosol and the internal store can be considered together as virtually one pool, which is refilled by the influx V_{in} and drained by the efflux $f(Z)$ (see also Fig. 1 in Knoke et al. 2008). At steady state, Eq. 6 leads to $V_{in} = f(Z)$. The steady-state concentration of cytosolic Ca^{2+} can be obtained by taking the inverse function of $f(Z)$:

$$Z_{ss} = f^{-1}(V_{in}). \quad (7)$$

The existence of at least one steady state requires that V_{in} intersects with $f(Z)$. Additionally it is reasonable to assume that $f(Z)$ is strictly monotonic increasing because non-monotonic kinetics have not been observed for Ca^{2+} efflux. Under this assumption, which is fulfilled for many rate laws, such as Michaelis–Menten and Hill kinetics, $f(Z)$ is an invertible function which precludes the existence of more than one steady state.

The average cytosolic Ca^{2+} concentration of the oscillating signal can be calculated by integration of Eq. 6 over one period T:

$$\int_0^T \left(\frac{d(Y+Z)}{dt}\right) dt = \int_0^T V_{in} dt - \int_0^T f(Z) dt. \quad (8)$$

Since, for periodic oscillations, $Z(T) = Z(0)$ and $Y(T) = Y(0)$, we have

$$\int_0^T \left(\frac{d(Y+Z)}{dt}\right) dt = 0. \quad (9)$$

Therefore, Eq. 8 simplifies to:

$$0 = \int_0^T V_{\text{in}} \mathrm{d}t - \int_0^T f(Z) \mathrm{d}t. \tag{10}$$

The second integral on the right-hand side is equal to the average of $f(Z)$ multiplied by T. Accordingly, Eq. 10 gives

$$0 = TV_{\text{in}} - T\langle f(Z)\rangle \tag{11}$$

$$\langle f(Z)\rangle = V_{\text{in}} = f(Z_{\text{ss}}). \tag{12}$$

Equation 12 is intuitively clear because the average efflux must equal the average influx, otherwise an accumulation or depletion would occur. Now we have to distinguish different cases according to whether $f(Z)$ is a strictly convex, convex, linear, concave or strictly concave function over the range of the oscillation amplitudes. Let us begin with the case of a strictly convex function. Then, due to Jensen's inequality,

$$f(\langle Z\rangle) < \langle f(Z)\rangle \tag{13}$$

holds. Together with Eq. 12, this implies

$$f(\langle Z\rangle) < V_{\text{in}}. \tag{14}$$

The average concentration of cytosolic Ca^{2+}, $\langle Z\rangle$, can be obtained here by taking the inverse function of $f(\langle Z\rangle)$. Since $f(Z)$ is strictly monotonically increasing, the order relation 14 is conserved and leads to

$$\langle Z\rangle < f^{-1}(V_{\text{in}}). \tag{15}$$

Due to Eq. 7, $f^{-1}(V_{\text{in}})$ is equal to the steady-state concentration of cytosolic Ca^{2+}, so that:

$$\langle Z\rangle < Z_{\text{ss}}. \tag{16}$$

This shows that for an efflux function following strictly convex kinetics, the average cytosolic Ca^{2+} concentration is lower compared to its corresponding concentration at the unstable steady state.

For non-strictly convex efflux functions, the derivation runs as above, with the difference that $f(\langle Z\rangle) \leq \langle f(Z)\rangle$, which leads to

$$\langle Z\rangle \leq Z_{\text{ss}}. \tag{17}$$

As for linear efflux functions, it is worth noting that Jensen (1906) described linear functions as a common limit case between convex and concave functions. Accordingly, for linear functions, $f(\langle Z\rangle) = \langle f(Z)\rangle$. Therefore, a linear efflux function results in $\langle Z\rangle = Z_{\text{ss}}$; the average cytosolic Ca^{2+} concentration there equals the Ca^{2+} concentration of the corresponding unstable steady state. (For an analytical derivation and a numerical illustration by means of the Somogyi–Stucki model, see Knoke et al. 2008).

For concave functions, the above derivation can easily be modified by inverting the order relation. This leads to

$$\langle Z\rangle \geq Z_{\text{ss}}. \tag{18}$$

with the strict inequality holding for strictly concave functions.

Numerical simulations by way of examples

As an illustrative example of the general model described by Eqs. 4 and 5, we here consider the Ca^{2+} oscillation model introduced by Somogyi and Stucki (1991). This model consists of Eqs. 4 and 5 with the CICR from the internal store described by a non-linear, Hill-like equation:

$$V_{CICR} = \frac{k_3 Y Z^4}{K^4 + Z^4}.$$

Besides, a passive leak efflux $V_{\text{leak}} = k_f Y$, a linear pumping rate $V_{\text{pump}} = k_2 Z$ into the internal store and $V_{\text{in}} = \text{const.}$ are assumed.

While in the original model, the efflux is assumed to obey a linear kinetics, we here modify the efflux in three alternative ways, notably by using (i) a strictly convex quadratic function, (ii) a strictly concave Michaelis–Menten kinetics and (iii) a Hill kinetics, involving both a convex and a concave part (for a simulation with the original Somogyi–Stucki model, see Knoke et al. 2008).

Case (i): Quadratic efflux kinetics:

$$f(Z) = kZ^2. \tag{19}$$

Figure 3a illustrates relation 16 by numerical calculations of the modified Somogyi–Stucki model.

Case (ii): Michaelis–Menten kinetics

The effect of strictly concave functions on the average Ca^{2+} concentration is illustrated in Fig. 3b by numerical calculations of a modified Somogyi–Stucki model with a saturation function:

$$f(Z) = \frac{V_{\max} Z}{K_S + Z}, \tag{20}$$

where K_S denotes the half-saturation constant. Figure 3b confirms the analytical result for concave functions given in relation 18.

Case (iii): Hill kinetics

So far we have reasoned about purely convex or concave functions, but what about a Hill kinetics,

$$f(Z) = \frac{V_{\max} Z^n}{K_S^n + Z^n}, \tag{21}$$

which has a convex and a concave part? ($n > 1$ is the Hill coefficient.) This question is biologically relevant because experimental data indicate that the Ca^{2+} extrusion in most cell types follows a Hill kinetics (Camello et al. 1996; Carafoli 1991a). We now modify the Somogyi–Stucki model by using such a kinetics term for the efflux with a Hill coefficient of $n = 3$ (according to results of Camello et al.

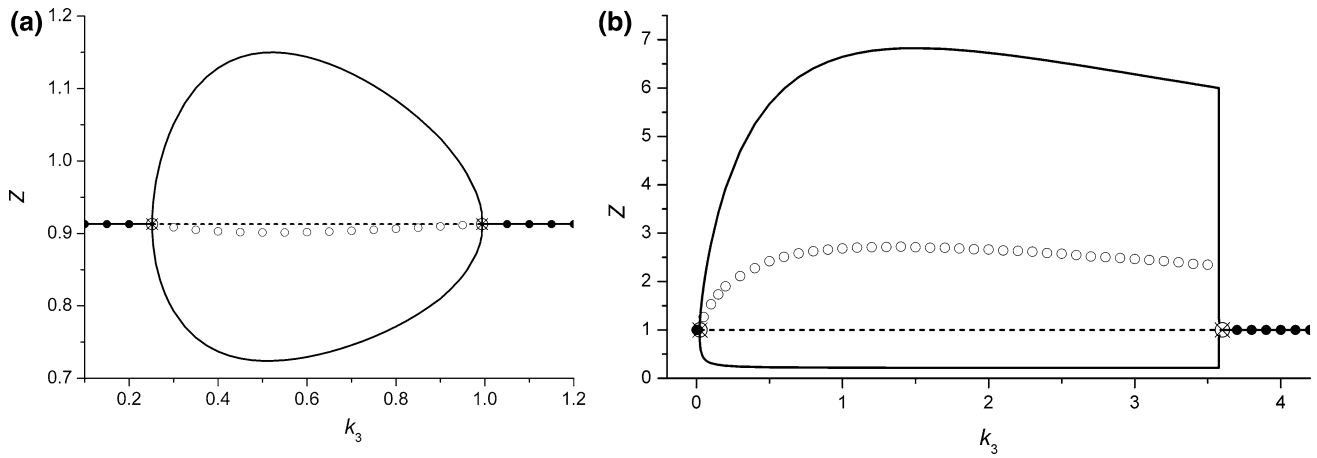

Fig. 3 Comparison of steady-state and average concentrations of cytosolic Ca^{2+} for two modified variants of the Somogyi–Stucki model, in which the efflux is a quadratic function, kZ^2 (**a**) or a Michaelis–Menten function, $V_{max}{*}Z/(K_S + Z)$ (**b**) of the cytosolic Ca^{2+} concentration. *Filled* (*empty*) *circles* average values in the steady-state (oscillatory) regime; *solid* (*dashed*) *horizontal line* stable (unstable) steady state; *curved lines* envelope of oscillations. Parameter values: $V_{in} = 1$, $k_2 = 2$, $K = 1$, $k_f = 0.01$; **a** $k = 1.2$; **b** $V_{max} = 1.2$, $K_S = 0.2$

1996). Numerical calculations indicate that the average Ca^{2+} concentration depends on the position of the K_S value between baseline and maximal peak height of the oscillation and on the shape of the peaks (spike-like or sinusoidal). The average Ca^{2+} concentration can be higher or lower than the corresponding steady-state value. These qualitative differences are due to the effect of the convex and concave part of the Hill kinetics. Figure 2b in Knoke et al. (2008) shows a numerical example. The oscillation shows a spike-like pattern in the predominant part of the parameter range, which resembles experimentally obtained peak shapes (e.g., see Somogyi and Stucki 1991). In that figure, it can be seen that the average cytosolic Ca^{2+} concentration is, with the parameter values used there, slightly above or close to the value at the unstable steady state. We will analyse the case of Hill kinetics in more detail in the next section.

Hill kinetics and spike-like oscillations

First it is worth mentioning that if the range of oscillation is entirely below the inflection point of the Hill kinetics, the crucial relation 13 is trivially fulfilled due to Jensen's inequality, since f is convex in this range. The inflection point of the Hill kinetics is given by:

$$Z_{ip} = K_S\left(\frac{n-1}{n+1}\right)^{1/n}, \tag{22}$$

as can be shown by equating the second derivative of Eq. 21 with zero. Interestingly, relation 13 can also be true if the peak extends beyond the inflection point into the concave part of the Hill kinetics. The relation still holds as long as the concave part does not outweigh the effect of the convex part. Whether or not this is the case depends on the signal shape and kinetic parameters. To analyse this theoretically, we will here consider a square-shaped Ca^{2+} signal, as has been done in earlier theoretical work (Li and Goldbeter 1992; Dupont et al. 2003; Marhl et al. 2006) to approximate the spike-like oscillation pattern seen in experiments. Then the efficiency of such Ca^{2+} oscillations depends on the fine-tuning of the baseline Z_1, peak amplitude Z_2 of the Ca^{2+} signal with respect to K_S and the ratio, $\gamma = T_p/T$, between peak width and period (Fig. 4a–c). The parameter γ $(0 \le \gamma \le 1)$ is called the duty ratio of the oscillation (Salazar et al. 2008). If the baseline or peaks are too high, the lowering of the average Ca^{2+} concentration is over-compensated (see Fig. 4b, c).

The square-shaped Ca^{2+} signal is described mathematically as:

$$Z(t) = \begin{cases} 0\,, t \bmod T > T_p \\ Z_2\,, t \bmod T \le T_p \end{cases} \tag{23}$$

(mod: modulo operator). First, the baseline Z_1 is set to zero, as has also been assumed in other theoretical studies (Marhl et al. 2006; Salazar et al. 2008). The general case of arbitrary Z_1, which leads to more cumbersome equations, is treated in Appendix A. The approximation $Z_1 = 0$ can be justified by the facts that experimental observations show baseline concentrations that are much lower than peak amplitudes and that these low (though non-zero) values do not contribute much whenever the binding of Ca^{2+} is cooperative (Hill coefficient $\geq$2).

Calculating the average of $Z(t)$ over one period gives:

$$\langle Z\rangle = \frac{1}{T}\int_0^T Z(t)\mathrm{d}t = \frac{T_P}{T}Z_2 = \gamma Z_2. \tag{24}$$

We can now analyse for which parameter values relation 13 holds (including the case of equality). With

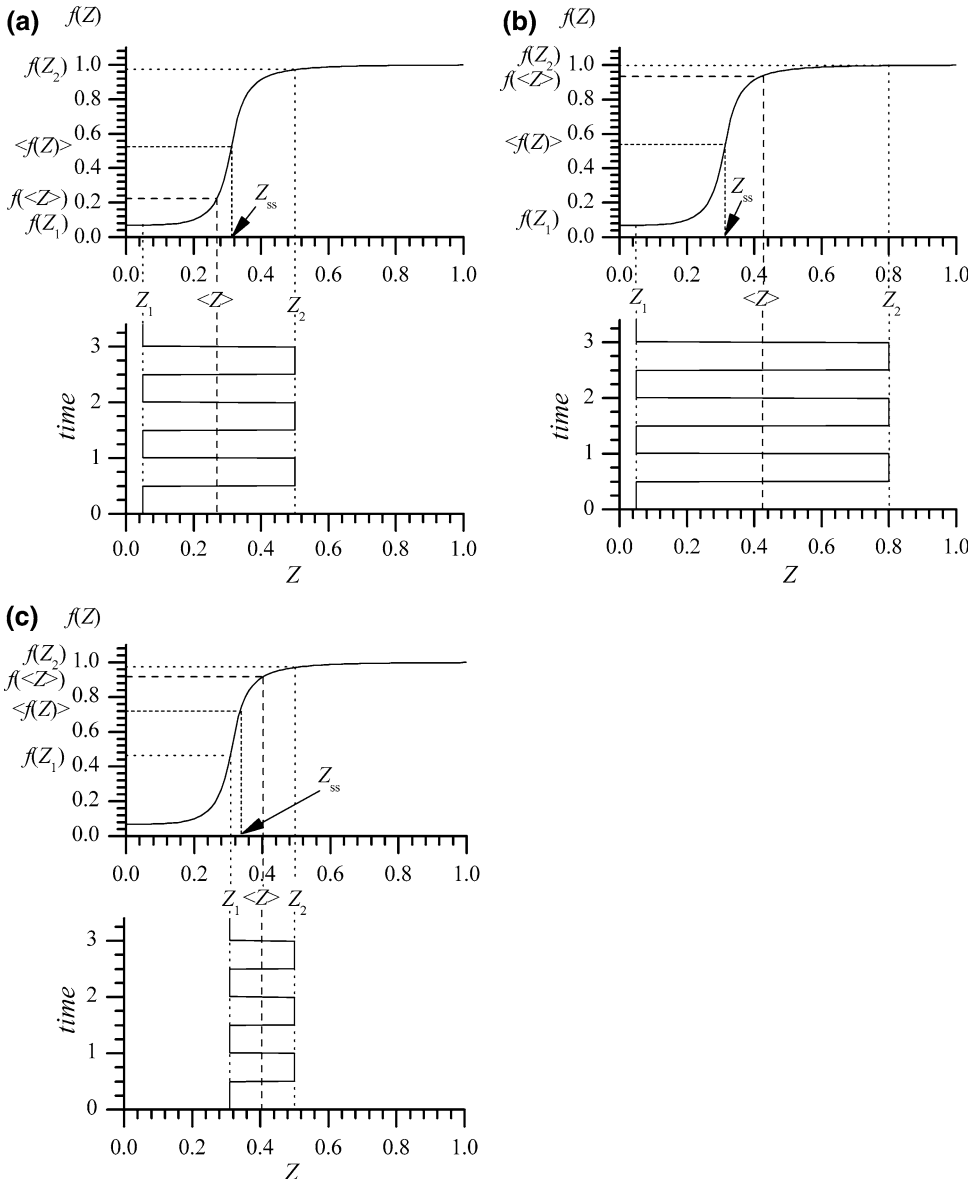

Fig. 4 Kinetics of the efflux of Ca^{2+} out of the cell aligned with the amplitude range $[Z_1, Z_2]$ of the Ca^{2+} spikes. The duration of the spikes is half a period of the signal ($\gamma = 0.5$). Z_{ss} denotes the steady-state value of cytosolic Ca^{2+}. **a** The peak (maximum value) is above the inflection point but sufficiently small to decrease the average Ca^{2+} concentration below the steady-state value. **b** The peak is that far above the inflection point or **c** the baseline is so high that the average Ca^{2+} concentration is above the steady-state value

$f(Z)$ being the Hill kinetics from Eq. 21, we obtain the following equation:

$$\frac{(\gamma Z_2)^n}{K_S^n + (\gamma Z_2)^n} \leq \gamma \frac{Z_2^n}{K_S^n + Z_2^n}, \tag{25}$$

which can be solved for Z_2:

$$Z_2 \leq Z_{\text{crit}} = K_S \left(\frac{1 - \gamma^{n-1}}{\gamma^{n-1} - \gamma^n} \right)^{1/n}. \tag{26}$$

This bound lies between $+\infty$ (if the duty ratio tends to zero) and $K_S(n-1)^{1/n}$ if γ tends to 1, as can be shown by l'Hôpital's rule. Interestingly, the latter limit is larger than the Z value, Z_{ip}, at the inflection point (cf. Eq. 22). For any given γ and n, the bound in Eq. 26 indicates the allowed maximal peak height of the signal to fulfil inequality 13 including the equality case (Fig. 5).

The root term in Eq. 26 is above 1 for true cooperativity ($n \geq 2$) and, thus, the protein catalysing the efflux may work above half-saturation during spikes, up to the threshold of Z_{crit} (see Fig. 4) and still guarantee the inequality $\langle Z \rangle < Z_{ss}$. Thus the amplitude range is no longer bounded by the inflection point of the Hill kinetics but may rise into the concave part depending on the duty ratio (narrowness of the calcium spike). The more narrow the spikes are, the more saturated the protein can operate.

Alternatively we may want to solve Eq. 25 for the duty ratio γ to obtain a bound on the shape of the Ca^{2+} signal and, thus, to analyse the sharpness of spikes. This leads to a polynomial of degree $n + 1$ in γ. By taking into account the trivial roots $\gamma = 0$ and $\gamma = 1$, we can derive the reduced polynomial $R(\gamma)$ of degree $n - 1$:

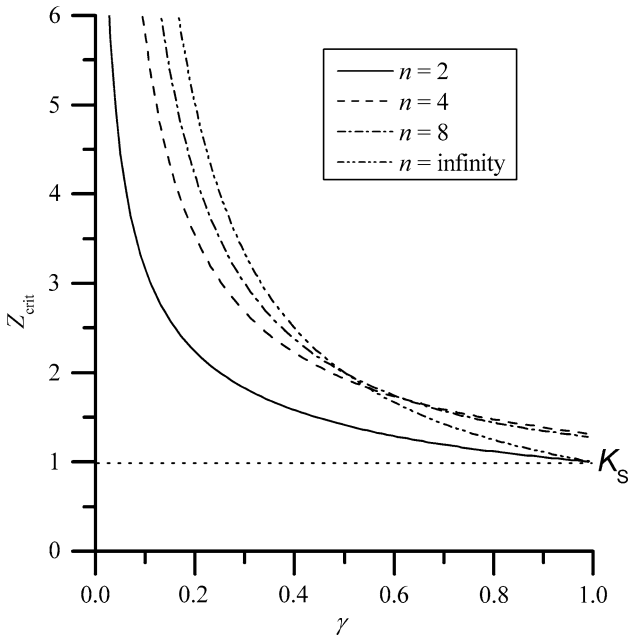

Fig. 5 Plot of the upper bound, Z_{crit}, on the peak height of square-shaped calcium spikes versus the duty ratio, γ, so that the average Ca^{2+} concentration is lower than, or equal to, the steady-state value, in the case where the efflux obeys Hill kinetics. *Curves* for various Hill coefficients n and $K_S = 1$ are shown. Note that Z values below K_S are always feasible as long as $n \geq 2$ and that, for $\gamma = 1$, there is a maximum of Z_{crit} at $n = 4.5911$

$$P(\gamma) = \gamma^{n+1} - (1 + \frac{1}{\mu^n})\gamma^n + \frac{1}{\mu^n}\gamma = R(\gamma)\gamma(\gamma - 1) = 0, \tag{27}$$

$$R(\gamma) = \gamma^{n-1} - \frac{1}{\mu^n}\left(\sum_{i=2}^{\lceil n \rceil} \gamma^{n-i} + \frac{\gamma^{n-\lceil n \rceil} - 1}{\gamma - 1}\right) = 0, \tag{28}$$

where we introduced, for simplification, the relative peak height $\mu = Z_2/K_S$. An analytical solution, which would correspond to the inverse of Eq. 26, is only possible for $n - 1$ less than, or equal to four (Abel–Ruffini theorem, cf. Fraleigh 1994).

For n a natural number the fraction in the second term disappears and we can give explicit solutions for $n \in \{2, 3, 4, 5\}$. The relevant solution for $n = 2$ is:

$$\gamma \leq \gamma_{crit,2} = \frac{1}{\mu^2} = \left(\frac{K_S}{Z_2}\right)^2. \tag{29}$$

We now consider the limit of $\gamma_{crit,n}$ as n tends to infinity. Computing the limit of Eq. 26 as n tends to infinity we obtain:

$$\lim_{n\to\infty} Z_{crit} = K_S \frac{1}{\gamma} \lim_{n\to\infty} \left(\frac{\gamma - \gamma^n}{1 - \gamma}\right)^{1/n} = K_S \frac{1}{\gamma} \lim_{n\to\infty} \left(\frac{\gamma}{1 - \gamma}\right)^{1/n}$$
$$= K_S \frac{1}{\gamma}, \tag{30}$$

which implies $\lim_{n\to\infty} \gamma_{crit,n} = 1/\mu$. From Fig. 5 we can see that $\gamma_{crit,2} \leq \gamma_{crit,n}$ for all $n > 2$. Thus, we can give a lower bound by $\gamma \leq (K_S/Z_2)^2$ for which inequality 25 always holds when we consider true cooperativity $n \geq 2$. We can see that the more saturated the Ca^{2+} pump works (high relative peak height), the duty ratio decreases more and thus the spikes have to be more narrow. Moreover, we derived from Eq. 26 that for γ tending towards unity we get $\mu = (n - 1)^{1/n}$. This term has a maximum at $n = 4.5911$, as has been noted in a study on the decoding of Ca^{2+} oscillations by Salazar et al. (2008). Thus, with Hill coefficients between 4 and 5, the duty ratio γ will have the widest range of allowed values (spike shapes) since it reaches $\gamma = 1$ for the highest relative saturation μ. This could be an advantage of the frequently found cooperativity of 4.

The analysis of the case with arbitrary baseline, Z_1 (Appendix A) shows that a low Z_1 value is advantageous for the convex effect of the Hill kinetics, as already anticipated from Fig. 4.

Comparison with experimental data

To compare our theoretical results with experimental data, we analysed time series of Ca^{2+} spikes given in three different studies (Fig. 6): on rat hepatocytes (Somogyi and Stucki 1991; Rooney et al. 1989) and gonadotroph cells (Li et al. 1994). To analyse the behaviour in dependence on a bifurcation parameter (e.g. hormone concentration), in a similar way as the numerical computations shown in Figs. 3a and 3b, we calculated the average Ca^{2+} concentration corresponding to different hormone concentrations from the oscillatory time series given in the figures of the publications. The lower and higher stable steady states that can be experimentally observed for low (or absent) and high hormone concentrations, respectively, are shown as well. These can be used to qualitatively interpolate the non-observable unstable steady state in the oscillatory range of the system. Although we do not know the exact dependence on the hormone concentration it is plausible to assume a smooth and monotonic dependence for this interpolation. We have used the time series given in Fig. 5 (with phenylephrine being the agonist) of Somogyi and Stucki (1991), Fig. 5 (gonadotropin-releasing hormone, GnRH) in Li et al. (1994) and the experimental records from Fig. 5 (vasopressin) of Rooney et al. (1989). As far as possible, we used the time points corresponding to the phase of sustained oscillations while we skipped transient spikes.

It can be seen that for the data shown in Fig. 6a, b, the steady state is nearly independent of the hormone concentration, whereas in Fig. 6c, it does depend on the hormone vasopressin. Quite surprisingly, the average of the oscillating cytosolic Ca^{2+} is clearly above the steady state in Fig. 6a, b, based on the above-mentioned interpolation.

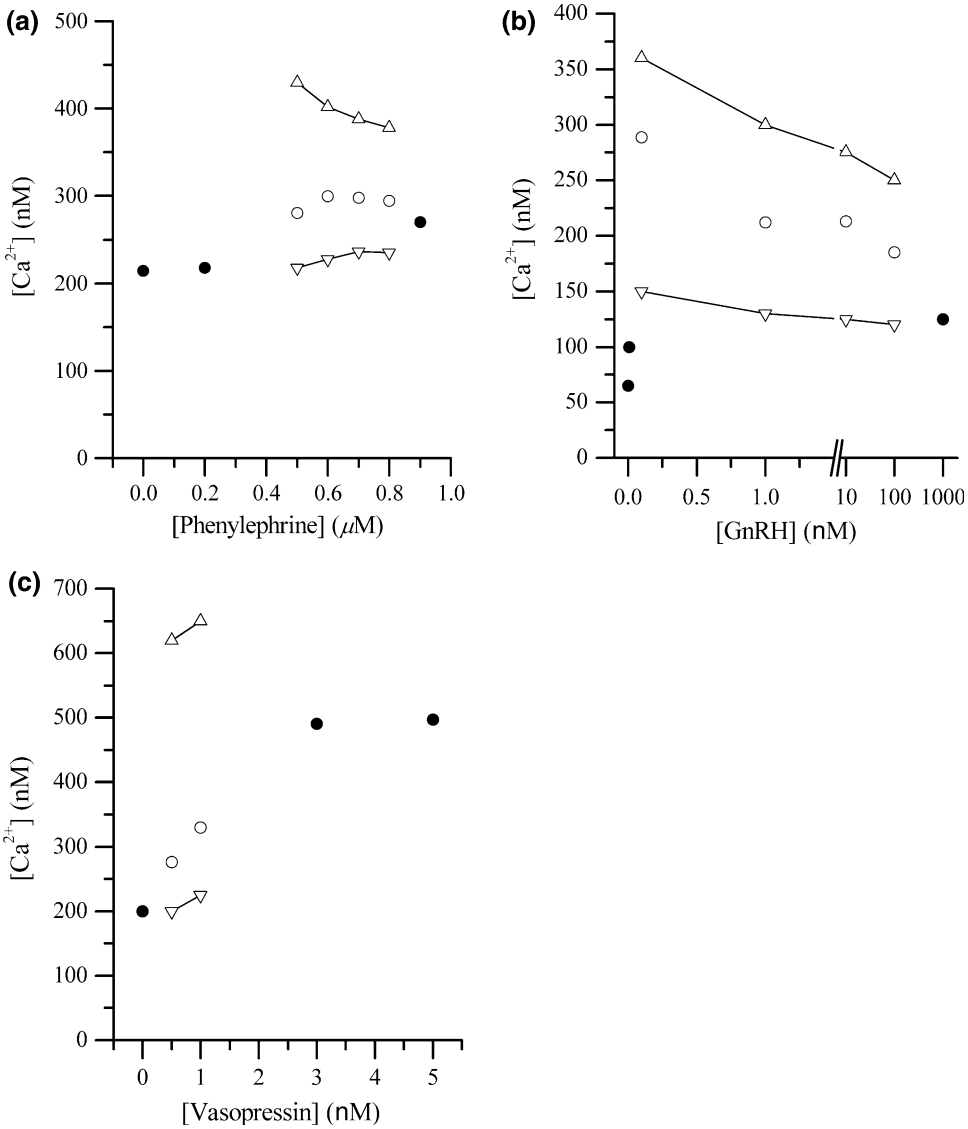

Fig. 6 Plotted results of the analysis of data from the studies by **a** Somogyi and Stucki (1991), **b** Li et al. (1994) and **c** Rooney et al. (1989). The figures in the cited work were binarised into a computer-readable matrix format. Since in Rooney et al. (1989), several resting periods had been generated by repeated washout, we normalised, in **c**, the time series to the same resting Ca^{2+} concentration (200 nM) observed before initial injection of hormone. *Filled* (*empty*) *circles* average values in the steady-state (oscillatory) regime; *triangles with connecting lines* envelope of oscillations. The two stable steady states (*filled circles*) on the left in **b** correspond to GnRH concentrations of 0 and 0.01 nM, respectively

For the vasopressin study in hepatocytes by Rooney et al. (1989), a monotonic increasing dependence of the steady state on the hormone concentration is observed (Fig. 6c). It was shown that vasopressin affects the influx of Ca^{2+} in a saturating fashion (Mauger et al. 1984). Therefore, a change of the steady-state concentration upon hormone variation can be accounted for in our model framework by a dependence of the Ca^{2+} influx V_{in} on the hormone concentration p. Although the inclusion of such effects does not change our derivation in the "General derivation" section, we can only speculate how vasopressin affects the steady-state concentration: The K_S value of the PMCA pump, for which magnitudes in the micromolar range were measured (Birch-Machin and Dawson 1988; Evers et al. 1988), could be significantly above the oscillation amplitude ($K_S \gg 700$ nM). This would limit the efflux to the first-order range of the putative concave efflux kinetics in hepatocytes, so that we obtain:

$$f(Z) \approx \frac{V_{max} Z}{K_S}. \tag{31}$$

Therefore, according to Eq. 7 the average and the steady state can be given as:

$$\langle Z \rangle \approx Z_{ss} \approx \frac{V_{in}(p) K_s}{V_{max}}. \tag{32}$$

The steady state is then a linear function of the influx, which is here dependent on the hormone concentration p. Thus, the dependence of the steady-state and average cytosolic Ca^{2+} concentrations on the hormone level would only be influenced by the kinetics of the influx function. Then, a saturating dependence of the influx on the hormone as experimentally observed (Mauger et al. 1984), could presumably describe the possibly saturating increase of the steady-state values calculated in Fig. 6c from experimental observations. In the case of such a saturating interpolation

in Fig. 6c, the average and steady-state values could coincide, which would be in agreement with the equality property due to a linear efflux.

Discussion

Using Jensen's inequality for the analysis of Ca^{2+} oscillations

For the Ca^{2+} oscillation signalling pathway, it has repeatedly been suggested that oscillations might lower the average Ca^{2+} concentration in the cytosol compared to a steady-state signal, so that harmful side effects can be avoided (Berridge 1989; Gall et al. 2000; Schuster et al. 2002). Here, we have analysed mathematically, by using Jensen's inequality, under which conditions such a decrease can occur. Jensen's inequality has been used earlier to analyse other biological questions, such as optimal body temperature (Martin and Huey 2008) or the development of a biologically variable ventilator to support lung-disease patients (Brewster et al. 2005).

We started from the conditions (a)–(c) given in the "Introduction" section (see also Knoke et al. 2008). Since the assumption of linear kinetics for the efflux was questionable in the light of experimental findings, we have relaxed condition (b) in that the influx is assumed to be independent of cytosolic Ca^{2+} (b1), while the efflux can be a non-linear function of that concentration. Models with non-linear efflux kinetics fulfilling conditions (a), (b1) and (c) are those proposed by Li et al. (1994), Höfer (1999) (when neglecting cell–cell coupling) and Sneyd et al. (2004).

We applied Jensen's inequality to examine the impact of different Ca^{2+} efflux functions (convex, linear and concave) on the relation between steady-state and average cytosolic Ca^{2+} concentrations. We could show that a strictly convex efflux function lowers the average concentration in comparison to the unstable steady state, whereas a strictly concave function increases it and a linear function results in equality. In this way we generalised our previous results (Knoke et al. 2008). Numerical simulation of a specific model similar to the Somogyi–Stucki model with different convex and concave efflux terms confirms the analytical results. Thus, oscillations have the potential of lowering the average Ca^{2+} concentration in the cytosol. A convex part in the efflux kinetics can, for example, be realised by cooperative binding of Ca^{2+} to the Ca^{2+} pumps in the plasma membrane. For different efflux kinetics, our method allows one to determine whether the average Ca^{2+} concentration is below or above the steady-state concentration. The shape of the efflux kinetics is certainly subject to changes in evolution. Two different processes need to be distinguished: the change in the efflux kinetics and the fine-tuning of parameters of, for example, the CICR to generate oscillations. Upon comparing the unstable steady state with the average in oscillations, we have in mind the latter process for a fixed shape of the efflux kinetics, so that the steady-state value does not change. This can then be done for various, fixed shapes.

Since the comparison is made with the unstable steady state, one might object that such states cannot be observed. However, as we showed here (see Eq. 7), for models fulfilling conditions (a), (b1) and (c), the value of the unstable steady state is even equal to the concentration at the stable stationary state for other parameter values, which allow stability. This holds for all parameters (for example, the hormone concentration) except those involved in the fluxes across the cell membrane because the steady-state concentration only depends on the latter parameters (Knoke et al. 2008). Our method is very helpful in giving an upper or lower bound on the average Ca^{2+} concentration since the stationary value can be calculated much more easily (often even analytically) than the average value.

For Hill kinetics, Jensen's inequality implies that the oscillation amplitude has to be in the convex part in order to lower the average concentration, if no special signal shape is assumed. Additionally, we performed a more detailed analysis using Hill kinetics for the efflux and the assumption of repetitive square-shaped Ca^{2+} spikes. For the average Ca^{2+} concentration to be lower than the corresponding steady state, the Ca^{2+} pumps may even work above half-saturation as long as the spikes are relatively narrow. This is expressed in inequalities derived here (relation 26 for the case of zero baseline and relation 38 for the general case), which represent conditions relating peak height, half-saturation constant, cooperativity factor and narrowness of the peaks. Especially the long-lasting baseline phase between peaks is likely to correspond to the convex part of the efflux function, therefore lowering the average Ca^{2+} concentration efficiently. A saturated operation of the Ca^{2+} pumps is preferable because then, during spikes, the cytosolic Ca^{2+} is pumped with the maximal velocity out of the cell into the extracellular medium, which is important in view of fast Ca^{2+} homeostasis (Berridge et al. 2003).

Models outside the scope of our study

Models that do not comply with conditions (a), (b1) or (c), cannot be analysed with our method. For example, the models developed by Marhl et al. (1997, 2000), Atri et al. (1993), Keizer and De Young (1994), and Li and Rinzel (1994) do not take into account influx nor efflux across the cell membrane and thus violate condition (a). Ca^{2+} in the endoplasmic reticulum (ER) is then no longer an

independent variable due to a conservation relation resulting from that assumption. The second variable needed for the emergence of oscillations is the Ca^{2+} bound to proteins (Marhl et al. 1997, 2000) or the active IP_3 receptor (Atri et al. 1993; Keizer and De Young 1994; Li and Rinzel 1994) rather than Ca^{2+} in the ER. However, it is also worth considering that neglecting the influx and efflux is a simplification in these models, while in reality such fluxes do occur. Condition (b1) is not fulfilled, for example, by the model proposed by Kummer et al. (2000), in which cytosolic Ca^{2+} affects a G-protein, which in turn influences the Ca^{2+} influx. Finally all models including store-operated Ca^{2+} release (for example, Li et al. 1997; Kowalewski et al. 2006) violate condition (c). However, since a lowering of the average concentration of cytosolic Ca^{2+} would have beneficial physiological effects, it is of interest to compare numerically the average and stationary concentrations in models not fulfilling one of the above conditions.

Analysing experimental data from the literature

To compare our theoretical results with experimental data, we analysed data on Ca^{2+} oscillation from three studies on rat hepatocytes (Somogyi and Stucki 1991; Rooney et al. 1989) and gonadotroph cells (Li et al. 1994). Perhaps surprisingly, the average values are higher than the steady-state values for the two data sets of Somogyi and Stucki (1991) and Li et al. (1994) (Fig. 6a, b). Gaspers and Thomas (2005) also investigated the effect of phenylephrine on hepatocytes. In Fig. 1 in that paper, both the steady-state Ca^{2+} concentration for low hormone and the average concentration for higher hormone levels are given. Assuming, in analogy to the similar study by Somogyi and Stucki (1991), that the steady-state Ca^{2+} concentration does virtually not depend on the agonist, one can deduce that the average is again above the steady state. The analysis of the data in the study by Somogyi and Stucki (1991) can be seen as representative for all hormones acting over the IP_3 signalling cascade in liver cells that do not affect the Ca^{2+} influx or efflux (for example a study on Bovine growth hormone by Marrero et al. 1996). Thus, it may be concluded that oscillations do not necessarily lower the cytosolic Ca^{2+} concentration. Moreover, our theoretical analysis predicts that both in hepatocytes and gonadotrophs the efflux function is a concave kinetics (i.e. a Michaelis–Menten kinetics) or, if it is a sigmoidal kinetics (i.e. a Hill function), then the oscillations amplitude range corresponds mainly to the concave part of the efflux function.

Although the data concerning the plasma membrane calcium ATPase (PMCA pump) in liver cells is less clear than in several other cell types (Delgado-Coello et al. 2006), in numerous studies on purified plasma membranes of rat liver enriched with the PMCA pump, it was shown that the Ca^{2+} efflux follows a concave Michaelis–Menten-like kinetics with a measured K_S ranging from 0.14 to 6 μM (Lin 1985; Birch-Machin and Dawson 1988; Evers et al. 1988; Kessler et al. 1990). The coincidence of the experimentally observed increase in the average Ca^{2+} concentration (Fig. 6a) and concavity of the efflux kinetics is in concordance with our theory.

In contrast to non-excitable cells, two Ca^{2+} transport systems are known to play a major role in excitable cells such as gonadotrophs: the PMCA pump and the Na^+/Ca^{2+} exchanger (Carafoli and Guerini 1993). The latter has low affinity for Ca^{2+} ($K_S \approx 1$ μM) but can transport bulk amounts of Ca^{2+}. Moreover, since it shows high cooperativity ($n = 4$), we can neglect the transport of the Na^+/Ca^{2+} exchanger in our considerations, since the amplitudes of the sustained oscillation in the time series from Li et al. (1994) are usually below 0.5 μM. For the PMCA pump we assume Hill kinetics similar to experimentally measured values for the erythrocyte pump as has also been done by Li et al. (1994) in their study ($n = 2$, $K_S = 0.3$ μM). Furthermore, the experimental time courses justify to assume square-shaped oscillations. For all hormone concentrations leading to sustained Ca^{2+} oscillations in this study the relative baseline α (with the property $0 \leq \alpha = Z_1/Z_2 < 1$) and the duty ratio γ of the oscillation are rather high (approximately 0.4 and >0.5, respectively). Thus, we can estimate from the

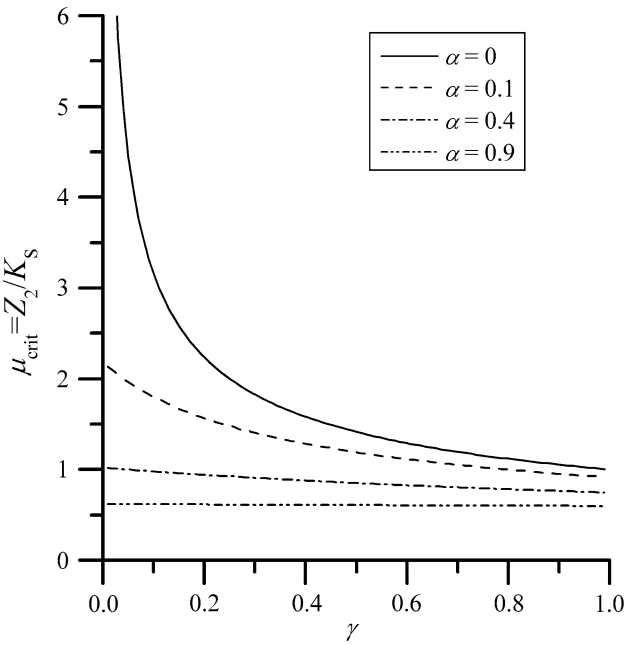

Fig. 7 Plot of the upper bound, μ_{crit}, on the relative peak height of square-shaped calcium spikes versus the duty ratio, γ, so that the average Ca^{2+} concentration is lower than the steady-state value, in the case where the efflux obeys a Hill kinetics. Curves for various relative baseline concentrations α are shown (with Hill coefficient $n = 2$ at a fixed value of Z_2). Note that the allowed range for μ decreases as the baseline increases

theoretical results obtained in the "Hill kinetics and spike-like oscillations" section (see Fig. 7) that the K_S value of 0.3 μM for the Hill kinetics is so small that the average is above the steady state. This is indeed observed in the analysis of the experimental data (Fig. 6b).

The data from Rooney et al. (1989) have been analysed, in a more speculative manner, in view of the dependence of the steady state on the hormone concentration. An efflux operating in the first-order range of a Michaelis–Menten kinetics of the hepatocyte PMCA pump and a saturating dependence of the influx on the agonist can explain the experimental observations. Interestingly, under these assumptions, the average and steady-state Ca^{2+} concentrations are likely to coincide, in agreement with our earlier theoretical prediction (Knoke et al. 2008).

However, additional experimental observations complicate the analysis of the data from Rooney et al. (1989). It was shown that the effect of vasopressin on the influx is (at least partially) due to store-operated Ca^{2+} channels (SOCs) (Rychkov et al. 2005). The opening of these SOCs and thus the influx of Ca^{2+} depends on a depleted concentration of Ca^{2+} in the ER, which is not taken into account by Eq. 32. Such a mechanism violates condition (c) in our assumptions, which precludes the application of our theory. Moreover, other studies also indicate an effect of vasopressin on the efflux through the PMCA pump (Prpić et al. 1984).

This shows that the situation is often more complicated than described in the models studied here. Besides theoretical analyses, further experimental work is needed to explain the effect of oscillations on the average cytosolic Ca^{2+} concentration. Our study points to the importance of such studies and may help to plan these experiments. As we could show, the relation between average and steady-state Ca^{2+} concentrations depends crucially on the type of the efflux kinetics and the parameters describing it (e.g. half-saturation constant and cooperativity). Therefore, the experimental determination of the aforementioned characteristics is of central importance. Moreover, it is important to measure the stable steady states both at low and high agonist concentrations.

Final remarks

Several possible explanations for the observation of an increased average Ca^{2+} concentration can be hypothesised. First, it may be sufficient if the Ca^{2+} concentration is below a critical threshold rather than to be minimised. Second, the average might not be lowered to avoid harmful stochastic effects, since relative fluctuations are higher when molecule numbers are lower. Interestingly, there are even positive stochastic effects, such as coherence resonance (Skupin et al. 2008). That random wave nucleation generates regular oscillations may require that Ca^{2+} concentrations are not too low, since Ca^{2+} is needed for the coupling of the independent excitable channel clusters.

Nevertheless, it may be argued that, although a certain increase in the average Ca^{2+} concentration is observed, several mechanisms prevent an excessive, harmful increase. One factor is the convex part of Hill efflux kinetics in some cells (cf. above). Another is the fact that Ca^{2+} peaks are usually very narrow (expressed above as a low duty ratio). This property is also important in the decoding of Ca^{2+} oscillations, which is usually performed by Ca^{2+}-binding proteins. Since the binding often obeys Hill kinetics, spikes contribute more than proportionally to protein activation. A promising extension of the present study in the future would be to analyse also that phenomenon by Jensen's inequality.

Acknowledgements We would like to thank E.G. Schukat-Talamazzini for support with the image analysis of time series and Ines Heiland for stimulating discussions. Financial support by the German Federal Ministry of Education and Research (BMBF) within the HepatoSys programme is gratefully acknowledged.

Appendix A: Analysis of the square-shaped signal with arbitrary baseline

The general square-shaped Ca^{2+} signal is given by:

$$Z(t) = \begin{cases} Z_1, t \bmod T > T_p \\ Z_2, t \bmod T \le T \end{cases}, \tag{33}$$

with the baseline $Z_1 < Z_2$. We can compute the average of $Z(t)$ over one period T as:

$$\langle Z \rangle = \frac{1}{T}\int_0^T Z(t)\mathrm{d}t = \gamma Z_2 + (1-\gamma)Z_1 = Z_2(\gamma + (1-\gamma)\alpha), \tag{34}$$

where we have introduced the relative baseline $0 \le \alpha = Z_1/Z_2 < 1$. Next we calculate the average of $f(Z(t))$ (f being the Hill kinetics from Eq. 21) over one period:

$$\langle f(Z) \rangle = \frac{1}{T}\int_0^T f(Z(t))\mathrm{d}t$$
$$= V_{\max}\left[\gamma\frac{Z_2^n}{K_S^n + Z_2^n} + (1-\gamma)\frac{(\alpha Z_2)^n}{K_S^n + (\alpha Z_2)^n}\right]. \tag{35}$$

From relations 13, 34 and 35, it follows:

$$\frac{Z_2^n(\gamma + (1-\gamma)\alpha)^n}{K_S^n + Z_2^n(\gamma + (1-\gamma)\alpha)^n} \le \gamma\frac{Z_2^n}{K_S^n + Z_2^n} + (1-\gamma)\frac{(\alpha Z_2)^n}{K_S^n + (\alpha Z_2)^n}. \tag{36}$$

Factoring out Z_2 on both sides and introducing the relative saturation $\mu = Z_2/K_S$, we can write:

$$\frac{(\gamma+(1-\gamma)\alpha)^n}{\frac{1}{\mu^n}+(\gamma+(1-\gamma)\alpha)^n} \le \gamma\frac{1}{\frac{1}{\mu^n}+1}+(1-\gamma)\frac{\alpha^n}{\frac{1}{\mu^n}+\alpha^n}. \quad (37)$$

This can be solved for μ:

$$\mu \le \mu_{\text{crit}} = \left(\frac{\alpha^n+\gamma(1-\alpha^n)-(\alpha+\gamma-\alpha\gamma)^n}{(1-\gamma(1-\alpha^n))(\alpha+\gamma-\alpha\gamma)^n-\alpha^n}\right)^{1/n}. \quad (38)$$

When plotting the allowed range of μ (the area below μ_{crit}) over γ as in Fig. 4, we can see that it decreases with increasing α (see Fig. 7 with $n = 2$). This corresponds to increasing the baseline concentration of Ca^{2+}.

References

Albrecht MA, Colegrove SL, Friel DD (2002) Differential regulation of ER Ca^{2+} uptake and release rates accounts for multiple modes of Ca^{2+}-induced Ca^{2+} release. J Gen Physiol 119:211–233

Atri A, Amundson J, Clapham D, Sneyd J (1993) A single-pool model for intracellular calcium oscillations and waves in the *Xenopus laevis* oocyte. Biophys J 65:1727–1739

Berridge MJ (1989) Cell signalling through cytoplasmic calcium oscillations. In: Goldbeter A (ed) Cell to cell signalling: from experiment to theoretical models. Academic Press, London, pp 449–459

Berridge MJ (1997) Elementary and global aspects of calcium signalling. J Exp Biol 200(Pt2):315–319

Berridge MJ, Bootman MD, Lipp P (1998) Calcium—a life and death signal. Nature 395(6703):645–648

Berridge MJ, Bootman MD, Roderick HL (2003) Calcium signalling: dynamics, homeostasis and remodelling. Nat Rev Mol Cell Biol 4(7):517–529

Birch-Machin MA, Dawson AP (1988) Ca^{2+} transport by rat liver plasma membranes: the transporter and the previously reported Ca^{2+}-ATPase are different enzymes. Biochim Biophys Acta 944(2):308–314

Borghans JM, Dupont G, Goldbeter A (1997) Complex intracellular Ca^{2+} oscillations: a theoretical exploration of possible mechanisms. Biophys Chem 66(1):25–41

Brewster JF, Graham MR, Mutch WA (2005) Convexity, Jensen's inequality and benefits of noisy mechanical ventilation. J R Soc Interface 2:393–396

Bruce JI, Straub SV, Yule DI (2003) Crosstalk between cAMP and Ca^{2+} signaling in non-excitable cells. Cell Calcium 34:431–444

Camello P, Gardner J, Petersen OH, Tepikin AV (1996) Calcium dependence of calcium extrusion and calcium uptake in mouse pancreatic acinar cells. J Physiol 490:585–593

Carafoli E (1991a) Calcium pump of the plasma membrane. Physiol Rev 71:129–153

Carafoli E (1991b) The calcium pumping ATPase of the plasma membrane. Annu Rev Physiol 53:531–547

Carafoli E, Guerini D (1993) Molecular and cellular biology of plasma membrane calcium ATPase. Trends Cardiovasc Med 3:177–184

Delgado-Coello B, Trejo R, Mas-Oliva J (2006) Is there a specific role for the plasma membrane Ca^{2+}-ATPase in the hepatocyte? Mol Cell Biochem 285(1–2):1–15

Dupont G, Goldbeter A (1993) One-pool model for Ca2+ oscillations involving Ca2+ and inositol 1,4,5-triphosphate as co-agonists for Ca2+ release. Cell Calcium 14:311–322

Dupont G, Goldbeter A (1998) CaM kinase II as frequency decoder of Ca^{2+} oscillations. Bioessays 20:607–610

Dupont G, Swillens S, Clair C, Tordjmann T, Combettes L (2000) Hierarchical organization of calcium signals in hepatocytes: from experiments to models. Biochim Biophys Acta 1498:134–152

Dupont G, Houart G, De Koninck P (2003) Sensitivity of CaM kinase II to the frequency of Ca^{2+} oscillations: a simple model. Cell Calcium 34:485–497

Dupont G, Combettes L, Leybaert L (2007) Calcium dynamics: spatio-temporal organization from the subcellular to the organ level. Int Rev Cytol 261:193–245

Evers C, Hugentobler G, Lester R, Gmaj P, Meier P, Murer H (1988) ATP-dependent Ca^{2+} uptake and Ca^{2+}-dependent protein phosphorylation in basolateral liver plasma membranes. Biochim Biophys Acta 939(3):542–550

Falcke M (2004) Reading the patterns in living cells—the physics of Ca^{2+} signalling. Adv Phys 53:255–440

Fraleigh JB (1994) A first course in abstract algebra. Addison Wesley Publishing Company, Reading, MA

Gall D, Baus E, Dupont G (2000) Activation of the liver glycogen phosphorylase by Ca^{2+} oscillations: a theoretical study. J Theor Biol 207:445–454

Gaspers LD, Thomas AP (2005) Calcium signaling in liver. Cell Calcium 38(3–4):329–342

Goldbeter A (1996) Biochemical oscillations and cellular rhythms. Cambridge University Press, Cambridge

Goldbeter A, Dupont G, Berridge MJ (1990) Minimal model for signal-induced Ca^{2+} oscillations and for their frequency encoding through protein phosphorylation. Proc Natl Acad Sci USA 87(4):1461–1465

Grubelnik V, Larsen AZ, Kummer U, Olsen LF, Marhl M (2001) Mitochondria regulate the amplitude of simple and complex calcium oscillations. Biophys Chem 94:59–74

Hardy GH, Littlewood JE, Pólya G (1988) Inequalities, 2nd edn. Cambridge University Press, Cambridge

Hauser MJB, Kummer U, Larsen AZ, Olsen LF (2001) Oscillatory dynamics protect enzymes and possibly cells against toxic substances. Faraday Discuss 120:215–227

Heinrich R, Schuster S (1996) The regulation of cellular systems. Chapman and Hall, New York

Höfer T (1999) Model of intercellular calcium oscillations in epatocytes: synchronization of heterogeneous cells. Biophys J 77:1244–1256

Houart G, Dupont G, Goldbeter A (1999) Bursting, chaos and birhythmicity originating from self-modulation of the inositol 1,4,5-trisphosphate signal in a model for intracellular Ca^{2+} oscillations. Bull Math Biol 61:507–530

Jacob R (1990) Calcium oscillations in electrically non-excitable cells. Biochim Biophys Acta 1052:427–438

Jensen JLWV (1906) Sur les fonctions convexes et les inégalités entre les valeurs moyennes. Acta Math 30:175–193

Keizer J, De Young G (1994) Simplification of a realistic model of IP3-induced Ca^{2+} oscillations. J Theor Biol 166:431–442

Kessler F, Bennardini F, Bachs O, Serratosa J, James P, Caride AJ, Gazzotti P, Penniston JT, Carafoli E (1990) Partial purification and characterization of the $Ca^{2(+)}$-pumping ATPase of the liver plasma membrane. J Biol Chem 265(26):16012–16019

Knoke B, Marhl M, Perc M, Schuster S (2008) Equality of average and steady-state levels in some nonlinear models of biological oscillations. Theory Biosci 127:1–14

Kowalewski JM, Uhlen P, Kitano H, Brismar H (2006) Modeling the impact of store-operated Ca^{2+} entry on intracellular Ca^{2+} oscillations. Math Biosci 204:232–249

Krantz SG (1999) Jensen's Inequality. §9.1.3 in Handbook of complex variables. Boston MA, Birkhäuser, p 118

Kummer U, Olsen LF, Dixon CJ, Green AK, Bornberg-Bauer E, Baier G (2000) Switching from simple to complex oscillations in calcium signaling. Biophys J 79:1188–1195

Li YX, Goldbeter A (1992) Pulsatile signaling in intercellular communication. Biophys J 61:161–171

Li YX, Rinzel J (1994) Equations for InsP3 receptor-mediated $[Ca^{2+}]_i$ oscillations derived from a detailed kinetic model: a Hodgkin-Huxley like formalism. J Theor Biol 166(4):461–473

Li YX, Rinzel J, Keizer J, Stojilkovic SS (1994) Calcium oscillations in pituitary gonadotrophs: comparison of experiment and theory. Proc Natl Acad Sci USA 91:58–62

Li Y, Stojilkovic S, Keizer J, Rinzel J (1997) Sensing and refilling calcium stores in an excitable cell. Biophys J 72:1080–1091

Lin SH (1985) Novel ATP-dependent calcium transport component from rat liver plasma membranes. The transporter and the previously reported (Ca^{2+}-Mg^{2+})-ATPase are different proteins. J Biol Chem 260(13):7850–7856

Marhl M, Schuster S, Brumen M, Heinrich R (1997) Modelling the interrelations between calcium oscillations and ER membrane potential oscillations. Biophys Chem 63:221–239

Marhl M, Haberichter T, Brumen M, Heinrich R (2000) Complex calcium oscillations and the role of mitochondria and cytosolic proteins. Biosystems 57:75–86

Marhl M, Perc M, Schuster S (2006) A minimal model for decoding of time-limited Ca^{2+} oscillations. Biophys Chem 120:161–167

Marrero I, Green AK, Cobbold PH, Dixon CJ (1996) Bovine growth hormone induces oscillations in cytosolic free Ca^{2+} in single rat hepatocytes. Biochem J 313(Pt 2):525–528

Martin TL, Huey RB (2008) Why "suboptimal" is optimal: Jensen's inequality and ectotherm thermal preferences. Am Nat 171:E102–E118

Mauger JP, Poggioli J, Guesdon F, Claret M (1984) Noradrenaline, vasopressin and angiotensin increase Ca^{2+} influx by opening a common pool of Ca^{2+} channels in isolated rat liver cells. Biochem J 221(1):121–127

Olsen LF, Hauser MJB, Kummer U (2003) Mechanism of protection of peroxidase activity by oscillatory dynamics. Eur J Biochem (FEBS) 270:2796–2804

Prpić V, Green KC, Blackmore PF, Exton JH (1984) Vasopressin-, angiotensin II-, and alpha 1-adrenergic-induced inhibition of Ca^{2+} transport by rat liver plasma membrane vesicles. J Biol Chem 259(3):1382–1385

Putney JW Jr (1998) Calcium signalling: up, down, up, down. What's the point? Science 279:191–192

Rapp PE, Mees AI, Sparrow CT (1981) Frequency encoded biochemical regulation is more accurate than amplitude dependent control. J Theor Biol 90(4):531–544

Rooney TA, Sass EJ, Thomas AP (1989) Characterization of cytosolic calcium oscillations induced by phenylephrine and vasopressin in single fura-2-loaded hepatocytes. J Biol Chem 264:17131–17141

Rychkov GY, Litjens T, Roberts ML, Barritt GJ (2005) ATP and vasopressin activate a single type of store-operated Ca^{2+} channel, identified by patch-clamp recording, in rat hepatocytes. Cell Calcium 37(2):183–191

Salazar C, Politi AZ, Höfer T (2008) Decoding of Ca^{2+} oscillations by phosphorylation cycles: analytic results. Biophys J 94(4): 1203–1215

Schuster S, Marhl M, Höfer T (2002) Modelling of simple and complex calcium oscillations. From single-cell responses to intercellular signalling. Eur J Biochem 69:1333–1355

Skupin A, Kettenmann H, Winkler U, Wartenberg M, Sauer H, Tovey SC, Taylor CW, Falcke M (2008) How does intracellular Ca^{2+} oscillate: by chance or by the clock? Biophys J 94(6):2404–2411

Sneyd J, Tsaneva-Atanasova K, Yule DI, Thompson JL, Shuttleworth TJ (2004) Control of calcium oscillations by membrane fluxes. Proc Natl Acad Sci U S A 101(5):1392–1396

Somogyi R, Stucki JW (1991) Hormone-induced calcium oscillations in liver cells can be explained by a simple one pool model. J Biol Chem 266:11068–11077

Szekely D, Brennan SC, Mun H-C, Conigrave AD, Kuchel PW (2009) Effectors of the frequency of calcium oscillations in HEK-293 cells: wavelet analysis and a computer model. Eur Biophys J 39:149–165

Thul R, Bellamy TC, Roderick HL, Bootman MD, Coombes S (2008) Calcium oscillations. Adv Exp Med Biol 641:1–27

Valant PA, Adjei PN, Haynes DH (1992) Rapid Ca^{2+} extrusion via the Na^{+}/Ca^{2+} exchanger of the human platelet. J Membr Biol 130(1):63–82

Woods NM, Cuthbertson KS, Cobbold PH (1986) Repetitive transient rises in cytoplasmic free calcium in hormone-stimulated hepatocytes. Nature 319(6054):600–602